SUPPORTING INFORMATION ACCOMPANYING:

Crystalline Bilayers Unzipped and Rezipped: Solid-State Reaction Cycle of a Metal-Organic Framework with Triple Rearrangement of Intralayer Bonds

Dariusz Matoga,*[a] Kornel Roztocki,[a] Manuel Wilke,[b] Franziska Emmerling,[b] Marcin Oszajca,[a] Magdalena Fitta,[c] Maria Bałanda[c]

[a]Faculty of Chemistry, Jagiellonian University, Ingardena 3, 30-060, Kraków, Poland
[b]BAM Federal Institute for Materials Research and Testing, Richard-Willstätter-Str. 11, 12489 Berlin, Germany
[c]Institute of Nuclear Physics, Polish Academy of Sciences, Radzikowskiego 152, 31-342 Kraków, Poland

E-mail: dariusz.matoga@uj.edu.pl

Contents:

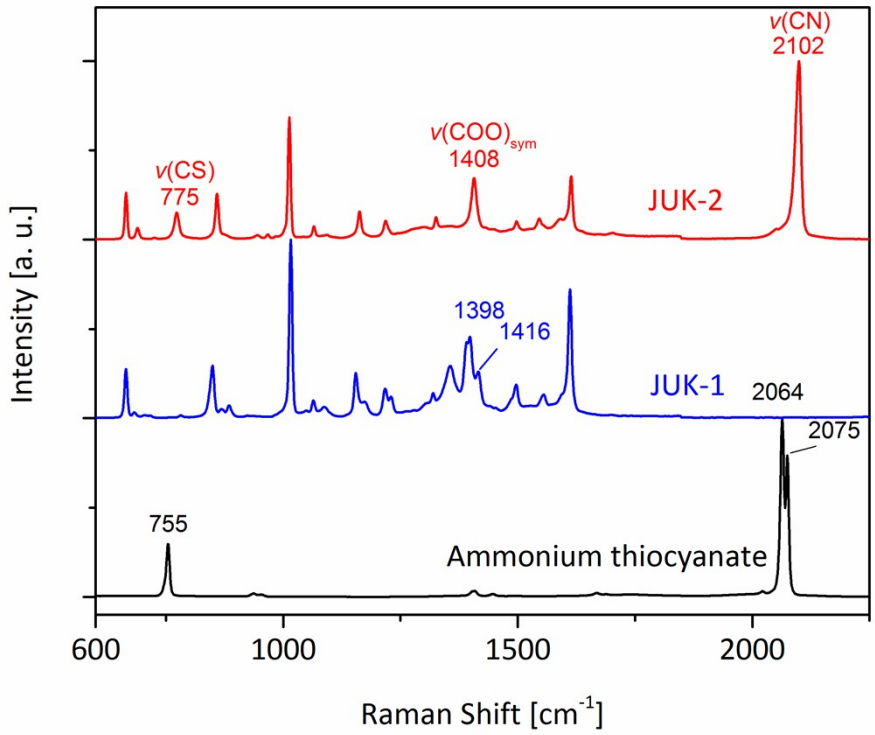

Figure S1. Raman spectra of ammonium thiocyanate, JUK-1 and JUK-2 (after *in situ* measurements: after neat grinding at 30 Hz) without the Perspex vessel. Numbers indicate selected Raman shifts in cm^{-1}.

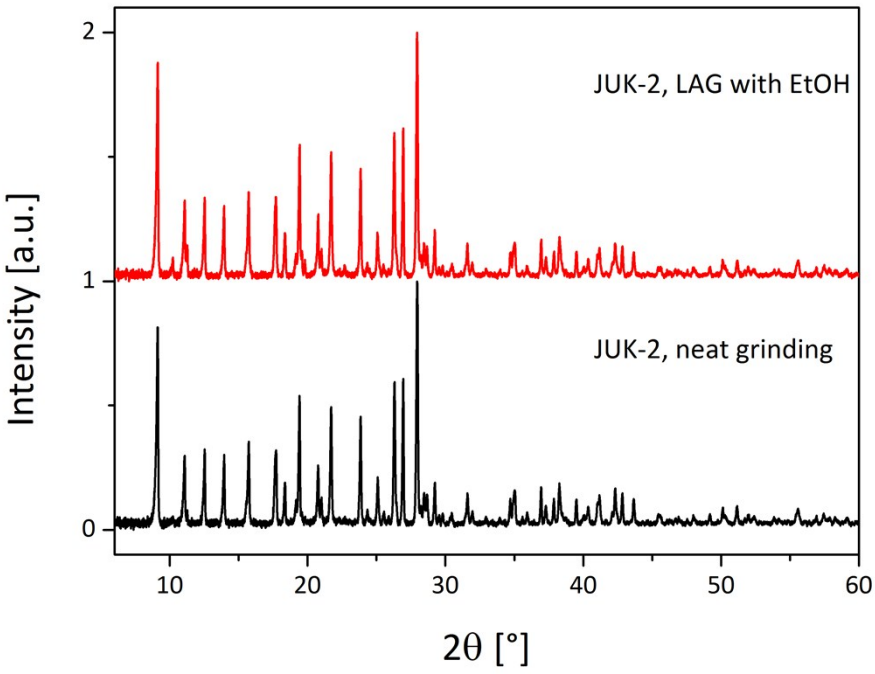

Figure S2. PXRD patterns recorded for the final products of JUK-2 after in situ measurements: after neat grinding (black) and after LAG with EtOH (red). Milling frequency: 30 Hz.

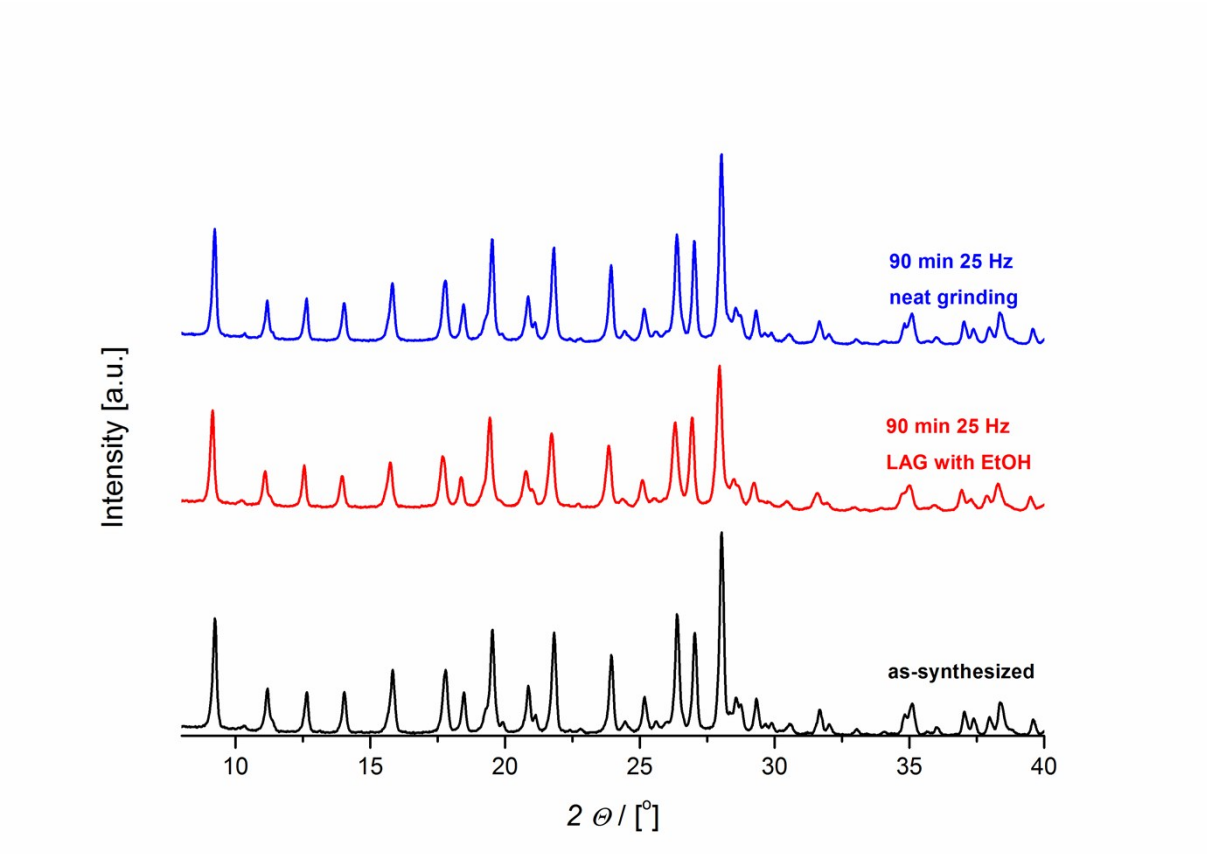

Figure S3. Stability tests for JUK-2. PXRD patterns recorded for JUK-2: as-synthesized (black), after neat grinding (blue) and after LAG with EtOH (red). Grinding was performed for 150 mg JUK-2 (and 150 μL EtOH in LAG) for 90 min in a vibration ball mill at 25 Hz (10 mL agate vessel and balls).

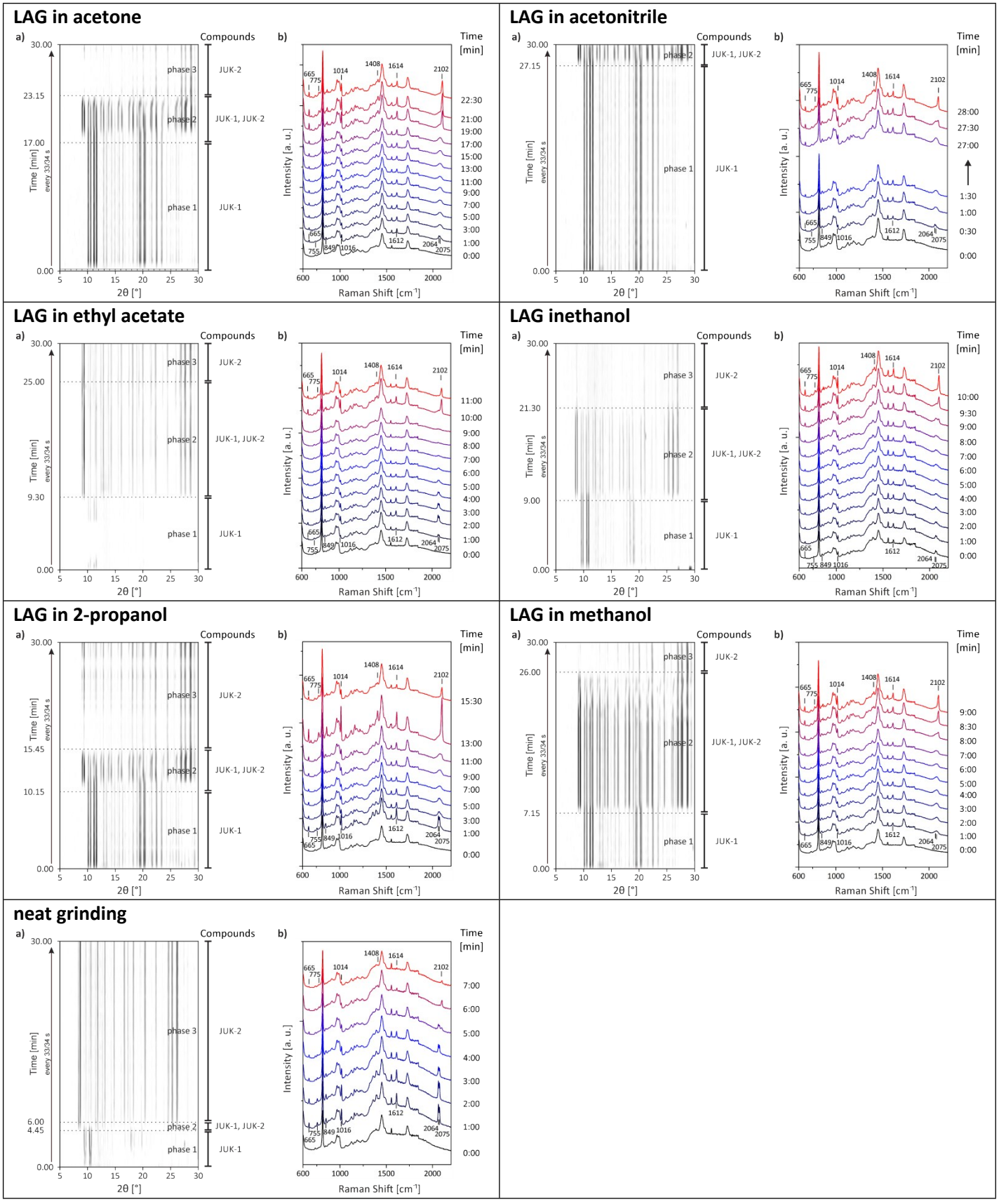

Figure S4. 2D plots of *in situ* synchrotron XRD data with a description of the detected compounds (a) and simultaneously acquired *in situ* Raman spectroscopy measurements (b) for the conversion of JUK-1 to JUK-2 as neat or liquid-assisted grinding (LAG) at various solvents at 30 Hz. Distinct bands other than originating from a Perspex vessel are indicated in the Raman spectra for the initial mixture and the final product. Milling conditions are given above the plots.

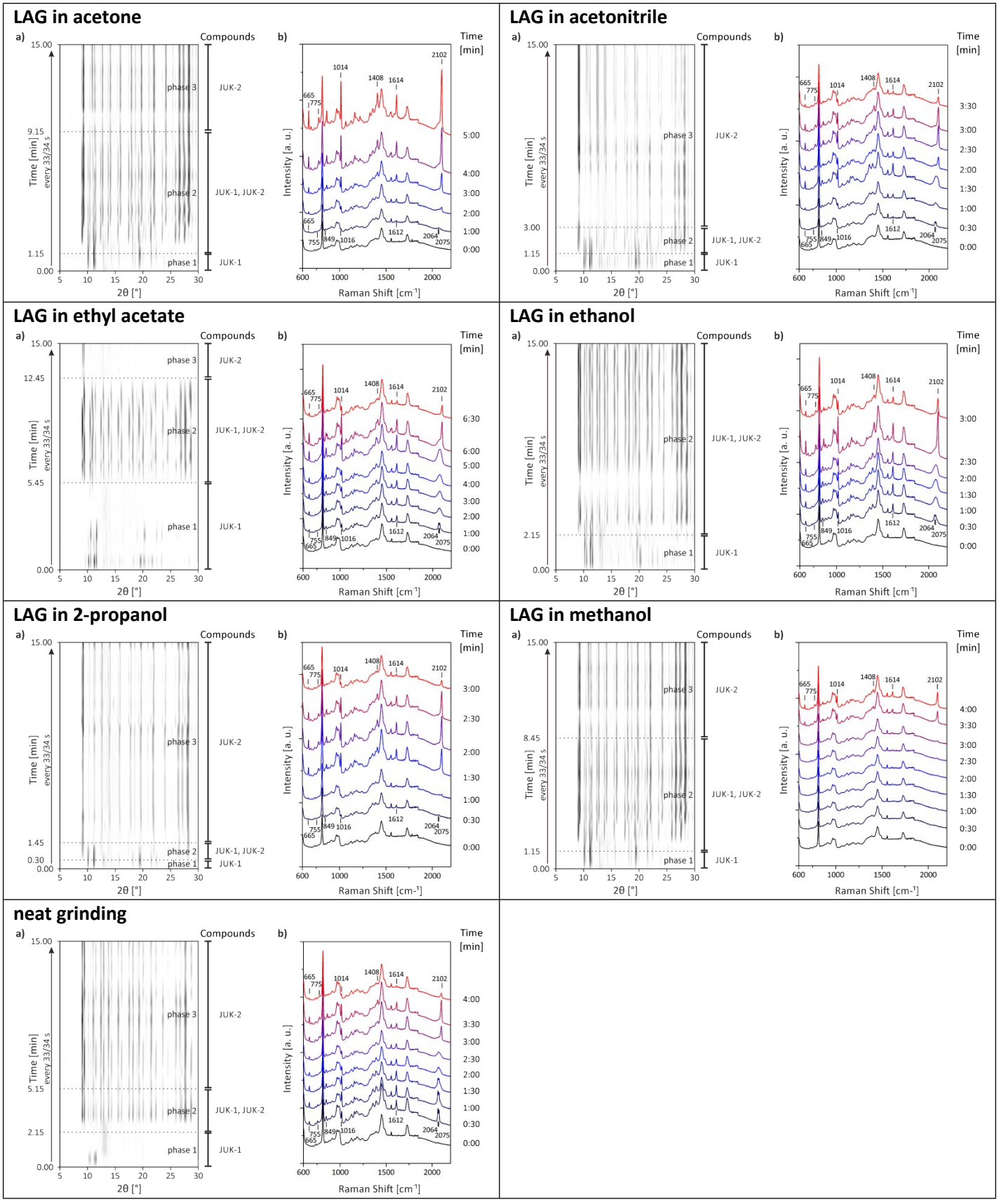

Figure S5. 2D plots of *in situ* synchrotron XRD data with a description of the detected compounds (a) and simultaneously acquired *in situ* Raman spectroscopy measurements (b) for the conversion of JUK-1 to JUK-2 as neat or liquid-assisted grinding (LAG) at various solvents at 50 Hz. Distinct bands other than originating from a Perspex vessel are indicated in the Raman spectra for the initial mixture and the final product. Milling conditions are given above the plots.

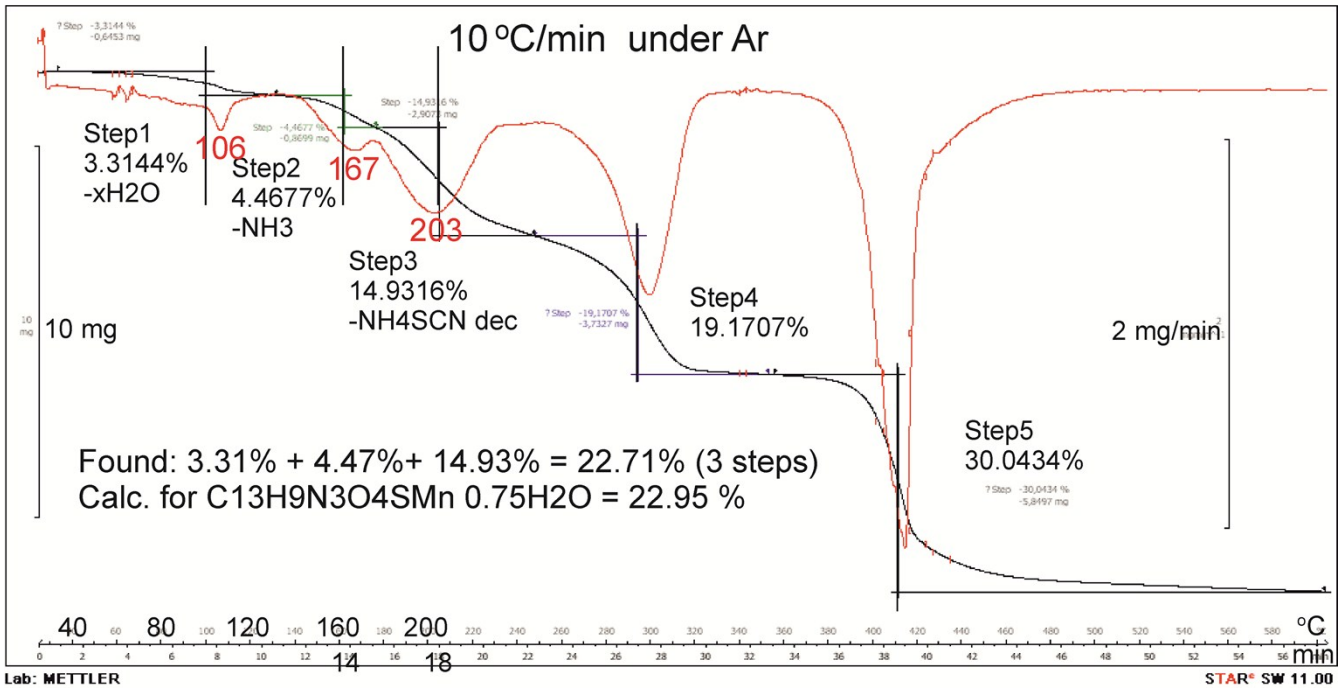

Figure S6. TGA (black) and dTGA (red) curves for $\{(NH_4)_2[Mn(ina)_2(NCS)_2]\}_n \cdot xH_2O$ (JUK-2) showing stepwise weight loss upon heating.

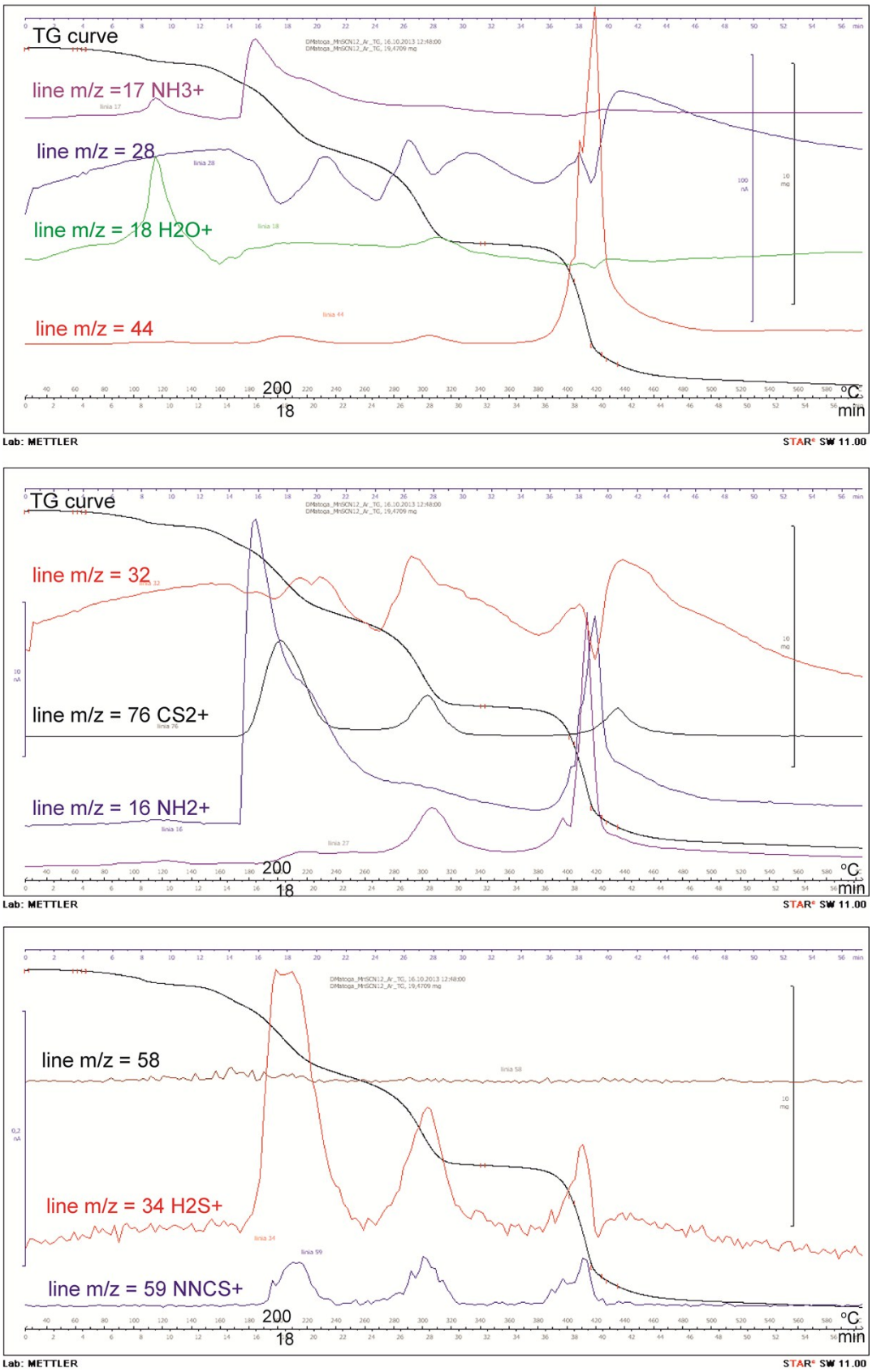

Figure S7. TGA (black) curves for $\{(NH_4)_2[Mn(ina)_2(NCS)_2]\}_n \cdot xH_2O$ (JUK-2) showing stepwise weight loss upon heating. Accompanying selected QMS (mass spectra) lines are given.

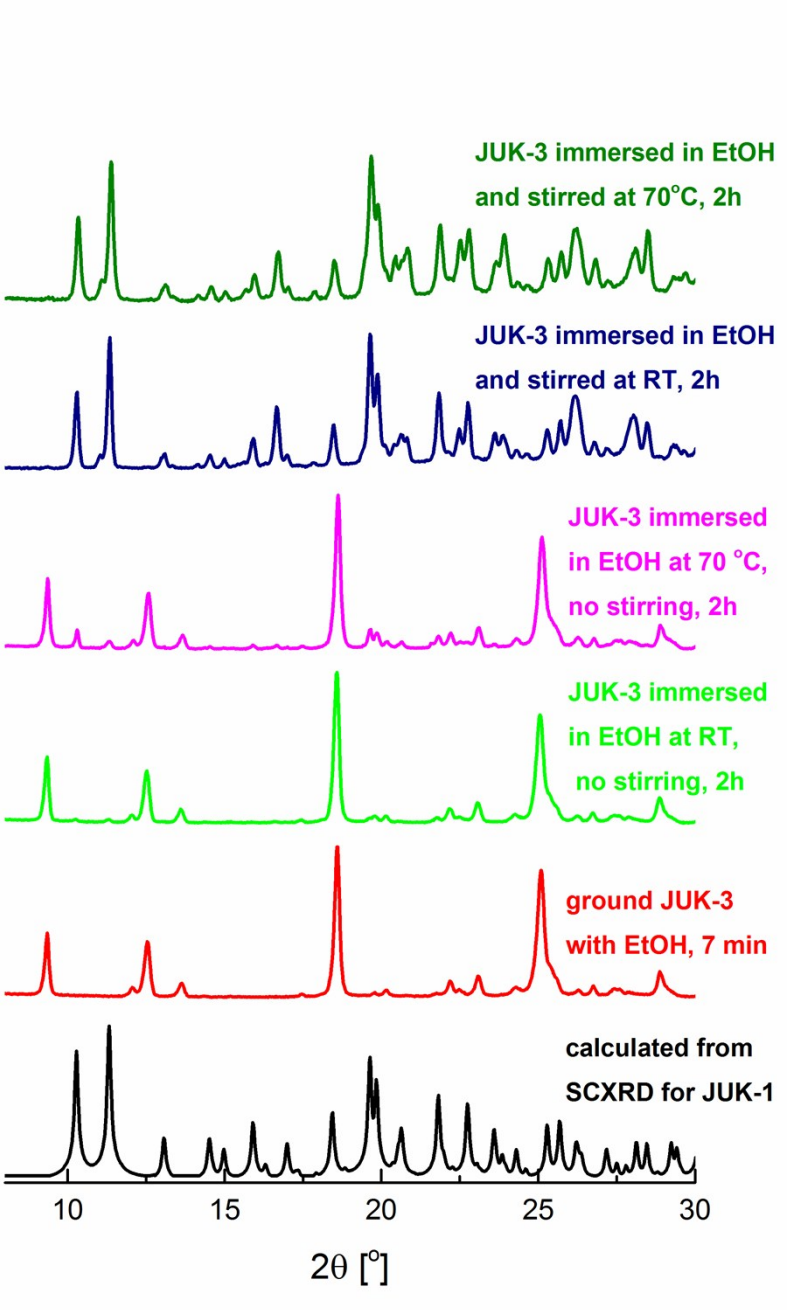

Figure S8. PXRD patterns of solids obtained after various control experiments to regenerate JUK-1 from JUK-3.

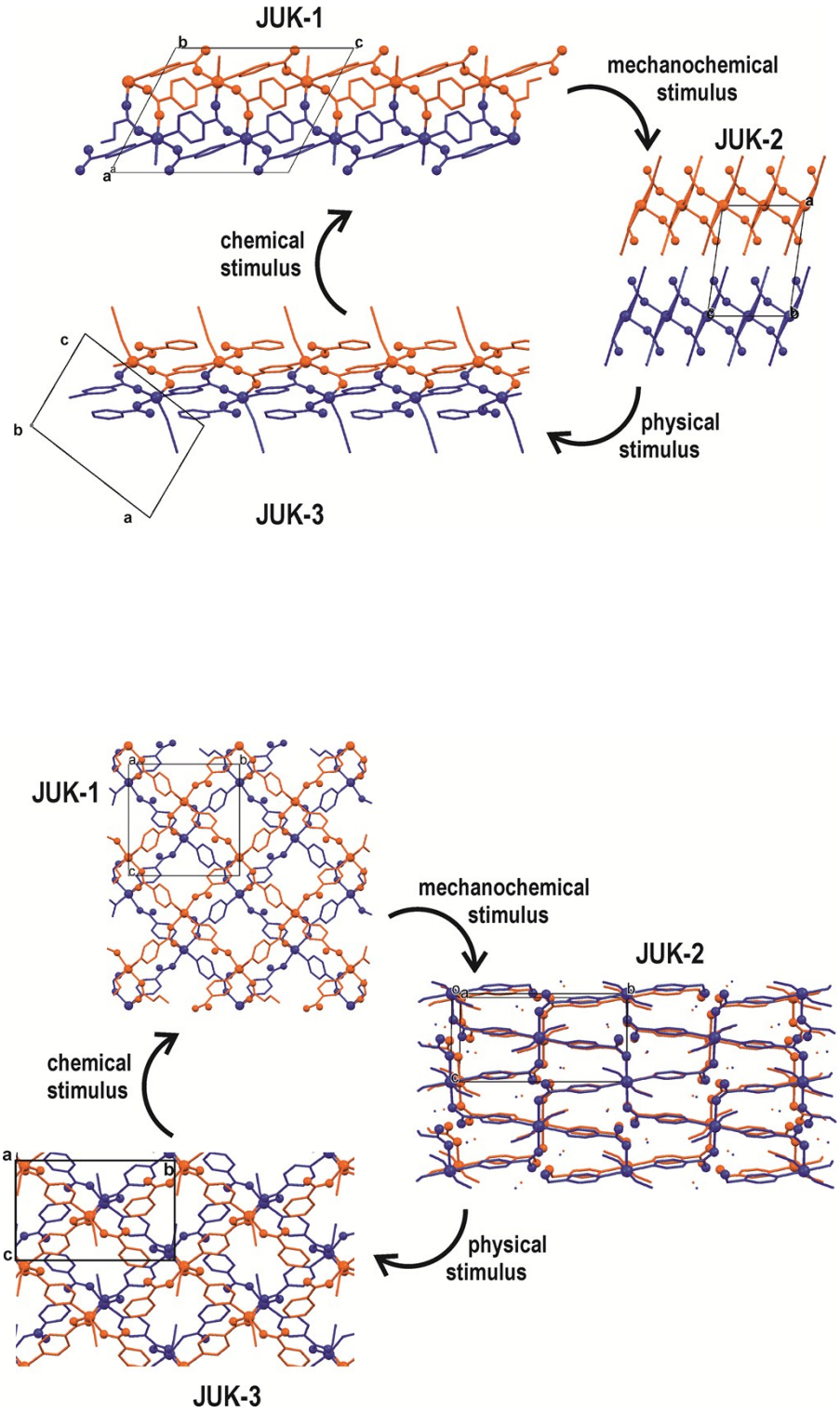

Figure S9. Structural details of the solid-state reaction cycle involving three 2D MOFs: JUK-1, JUK-2 and JUK-3 with triple rearrangement of intralayer isonicotinate ligands (two various views). Adjacent layers of JUK-2 and their position before the initial JUK-1 bilayer unzipping and after zipping to JUK-3 are indicated in orange and blue. Mn and carboxylate O atoms are shown as spheres. H atoms are omitted.

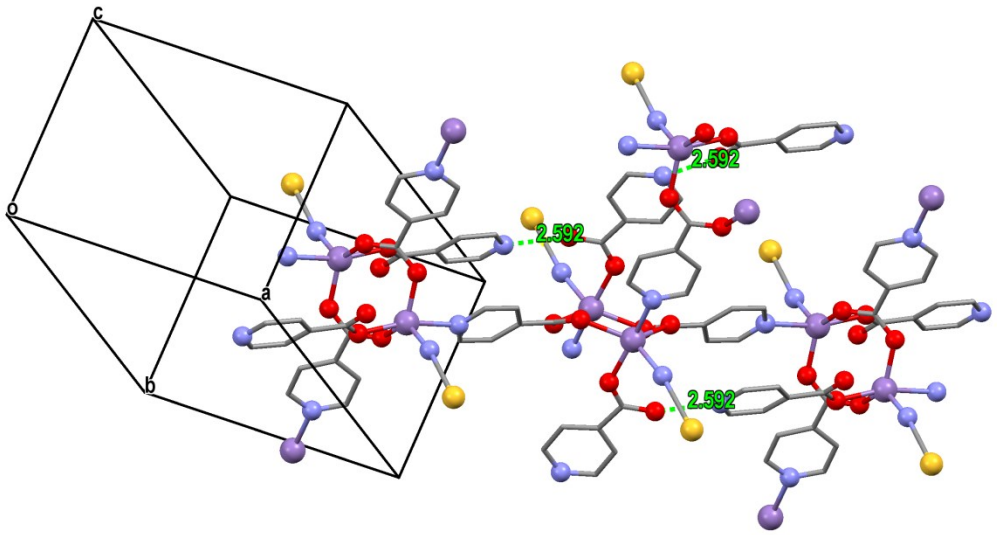

Figure S10. Partial view of JUK-3 structure with O···H···N hydrogen bonds between protonated isonicotinates (coordinated in a monodentate mode) shown as dashed green lines. Donor-acceptor distances O···N are indicated in Å. H atoms omitted, all non-C atoms are shown as spheres. Mn – purple, O – red, N– blue, S – yellow, C – grey.

Table S1. Data collection and structure refinement details for JUK-3, compared with other MOFs from the reaction cycle (JUK-1 and JUK-2).

	JUK-1	**JUK-2**	**JUK-3**
method	single-crystal XRD	powder XRD	powder XRD
instrument	Oxford Diffraction SuperNova CCD	PANalytical X'Pert PRO MPD	PANalytical X'Pert PRO MPD
empirical formula	$C_{14}H_{16}MnN_2O_6$	$C_{14}H_{16}MnN_6O_4S_2$	$C_{13}H_8MnN_3O_4S$
formula weight (g/mol)	363.23	451.4	357.2
crystal system	monoclinic	monoclinic	monoclinic
space group	P 2_1/c	P 2_1/c	P 2_1/n
a (Å)	10.869(5)	9.723(3)	12.4443(6)
b (Å)	12.130(5)	14.061(4)	13.9144(7)
c (Å)	13.783(4)	7.1516(18)	8.8461(3)
α (deg)	90.00	90	90
β (deg)	117.75(2)	97.92(3)	97.272(3)
γ (deg)	90.00	90	90
V (Å^3)	1608.2(11)	968.4(5)	1519.42(12)
Z	4	2	4
T (K)	293	293	453
d_{calc} (Mg/m^3)	1.500	1.5475	1.5616
μ (mm^{-1})	6.974	7.86	8.55
F(000)	748	458	720
wavelength (Å)	1.5418	1.5418	1.5418
crystal size (mm)	0.44 x 0.25 x 0.15	-	-
range for data collection (°)	$4.6 \leq \theta \leq 71.3$	$3.02 \leq 2\theta \leq 84.98$ with 0.02 step	$6.00 \leq 2\theta \leq 84.98$ with 0.02 step
index ranges	$-13 \leq h \leq 13$	-	-
	$-14 \leq k \leq 14$	-	-
	$-16 \leq l \leq 16$	-	-
reflections collected	22994	-	-
number of points	-	4099	3950
completness to θ (%)	99.2	-	-
max/min transmission	1.000/0.281	-	-
refinement method	full-matrix least-squares on F^2	Rietveld refinement	Rietveld refinement
data/restrains/parameters	3093/1/210	4099/19/65	3950/29/95
GOF	0.901	3.18	4.36
R indices	$R_1 = 0.0366$ (all data)	$R_p = 0.0645$	$R_p = 0.0453$
	w$R_2 = 0.0867$ (all data)	$R_{wp} = 0.0921$	$R_{wp} = 0.0687$
	$R_1 = 0.0329$ ($I > 2\sigma$)	$R = 0.1021$ ($I > 2\sigma$)	$R = 0.0748$ ($I > 2\sigma$)
	w$R_2 = 0.0832$ ($I > 2\sigma$)	$R_w = 0.1131$ ($I > 2\sigma$)	$R_w = 0.0741$ ($I > 2\sigma$)
largest diff. peak/hole (e/Å^3)	0.413/-0.362	0.57/-0.93	-